Unveiling corrosion inhibition properties of the *Cupressus Arizonica* leaves essential oil for carbon steel in 1.0 M HCl

S. Cherrad,[1,2]* I. Jaouadi,[1,2] Y. El Aoufir,[3,4] M. Tiskar,[1] B. Satrani,[2] M. Ghanmi,[2] A. Guenbour[4] and A. Chaouch[1]

[1]*Laboratory of Agro-Physiology, Biotechnologies, Environment and Quality, Department of Biology, Faculty of Sciences, University Ibn Tofail, Kenitra, Morocco*
[2]*Forest Research Center B.P 763, Rabat Agdal, 10050, Morocco*
[3]*Laboratory of Advanced Materials and Process Engineering, Higher School of Education and Training, Ibn Tofail University, PB 133-14050, Kenitra, Morocco*
[4]*Laboratory of Nanotechnology, Materials & Environment, Faculty of Sciences, Mohammed V University in Rabat, Morocco*
**E-mail: sara.cherrad@gmail.com*

Abstract

Corrosion scientist/engineers are showing great research interest in developing green corrosion inhibitors of plant origin. It has been reported that plant extracts possess good inhibitive characteristics, with little or no negative impact on the environment. In this work, accurate identification of the *Cupressus arizonica* leaves essential oil (CAEO) was obtained by hydrodistillation. Gas chromatography-mass spectrophotometer (GCMS) was used to identify its chemical constitution, which indicated the presence of 21.27%, 19.88%, 9.39%, 5.84% and 4.76% of *cis*-muurola-4(14),5-diene, terpin-4-ol, α-Pinene, δ-cadinene and *epi*-α-muurolol, respectively. The corrosion inhibition properties of CAEO for carbon steel (CS) in 1.0 M HCl were evaluated using weight loss measurements, potentiodynamic polarization, and electrochemical impedance spectroscopy (EIS). Results revealed that *Cupressus arizonica* leaves essential oil (CAEO) has an excellent inhibiting effect on the CS in 1.0 M HCl solution. The protection efficiency increases with increasing inhibitor concentration to attain 95% at 500 ppm. Potentiodynamic polarization studies revealed that CAEO acts primarily as a mixed-type inhibitor. The effect of temperature on the corrosion inhibition properties indicated a decrease in the inhibition efficiency from 92% (298 K) to 72% (328 K). Electrochemical impedance spectroscopy measurements showed that adsorbed molecules of CAEO formed a protective film on the carbon steel surface in 1.0 M HCl.

Keywords: *corrosion inhibition; Cupressus arizonica; carbon steel; essential oil; electrochemical techniques.*

Received: April 17, 2020. Published: May 20, 2020 doi: 10.17675/2305-6894-2020-9-2-15

1. Introduction

Corrosion is a fundamental process playing an essential role in economics and safety, particularly for metals [1, 2]. The use of inhibitors is one of the most practical methods for

protection against corrosion, especially in acidic media [3]. Most inhibitors used in industry are organic compounds primarily composed of nitrogen, oxygen and sulfur atoms. Inhibitors containing double or triple bonds play an essential role in facilitating the adsorption of these compounds onto metal surfaces [4–6]. A bond can be formed between the electron pair and/or the π-electron cloud of the donor atoms and the metal surface, thereby reducing corrosive attack in an acidic medium [7, 8]. Some of these organic compounds are toxic to humans, have a terrible environmental effect and high-cost [9]. The use of plant essential oils as an alternative to synthetic corrosion inhibitors has attracted keen interest in the past years [9–17]. Most plant essentials oils possess antibacterial activity and are low-cost products, which are the main advantages of corrosion inhibitors. Up till now, many essentials oils were used as effective corrosion inhibitors for iron or steel in acidic media, such as *Thyme Vulgaris* [18], *Lavande (Lavandula Dentata)* [19], *Limbarda crithmoides* [20], *Ammodaucus leucotrichus* [21]. The inhibition performance of plants extracts is usually ascribed to the presence of complex organic species, including tannins, alkaloids and nitrogen bases, carbohydrates and proteins as well as hydrolysis products in their composition. These organic compounds usually contain polar functions with nitrogen, sulfur, or oxygen atoms and have triple or conjugated double bonds or aromatic rings in their molecular structures, which are the major adsorption centers.

The objective of the present work is to investigate the inhibition effect of CAEO on the corrosion of carbon steel in 1.0 M hydrochloric acid by weight loss measurements, potentiodynamic polarization (PDP), electrochemical impedance spectroscopy (EIS) methods. The temperature effect and activation parameters were also investigated.

2. Materials and Methods

2.1. Plant collection and essential oil extraction

The leaves of *Cupressus arizonica* were harvested in March 2017 from Azrou (the Middle atlas of Morocco). Fresh vegetal material (boughs) was water distillated during 3 h using a Clevenger-type apparatus according to the method recommended by European Pharmacopoeia [22].

2.2. Components identification

The type of the device is as follows: Perkin Elmer Auto System XL, equipped with a detector of flame ionization (FID). 0.2 µl of EO are injected with a micro-syringe. Nitrogen (N_2) was used as a vector gas at a flow rate of 1 mL/min. The column used is a capillary. The column is of Elite type (60 m×0.320 mm), the thicknesses of the film is 1.0 µm, the hydrogen flow rate is (H_2) 35 mL/min, the synthetic air flow is 350 mL/min, the temperature of the injection is 235°C, the detection temperature is 240°C. The programming of the column temperature is the initial injection temperature which is 50°C for 5 min which then rises in increments of 4°C/min at 230°C for 5 min.

2.3. Materials preparation and solutions

The material used throughout the experiments is carbon steel with the following chemical composition in (wt. %) of 1.68% C, 0.65% N, 0.10% Na, 0.07% Mg, 0.39% Cr, 0.69% Mn and the remainder iron (Fe). The molar hydrochloric acid, used as an acid solution, was prepared by dilution of an Analytical Grade 37% HCl with double distilled water. The solution tests were freshly prepared before each experiment. The essential Oil of plant was dissolved in pure ethanol; adding the oil directly to the acid solution by gentle mechanical agitation for 1 h. Tests were carried out in triplicate to ensure reproducibility. Before all measurements, the exposed area of CS samples was mechanically abraded with (160 to 1200) grades of emery papers. The specimens were washed thoroughly with bidistilled water, degreased with ethanol and dried with hot air.

2.3. Electrochemical tests

Potentiodynamic Polarization (PDP) measurements were carried out in a conventional three-electrode electrolytic cell. Saturated calomel electrode (SCE) and platinum were used as a reference and auxiliary electrodes, respectively. The working electrode (carbon steel) was in parallelepiped form with a surface of 1 cm^2. These electrodes were connected to Voltalab (PGZ 300) piloted by a personal computer associated with Origa Master (Version 5) software. The scan rate was 1 mV/s started from an initial potential of –800 to –200 mV relative to the OCP. Before recording each curve, samples were subjected to open circuit corrosion in the electrolyte for 30 min, during which the system attained a stable open circuit potential (OCP). Corrosion current densities were obtained from the polarization curves by linear extrapolation of Tafel curves.

Electrochemical impedance spectroscopy (EIS) measurements were carried out with the same equipment used for the polarization measurements, leaving the frequency response analyzer out of consideration. After the determination of steady-state current at a given potential, EIS measurements were performed using an AC signal at a frequency range of 0.01 Hz to 100 kHz and 10 mV amplitude. The impedance diagrams were given in the Nyquist and Bode representations.

2.4. Weight loss measurement

Gravimetric measurements were carried out in glass bottle. After being weighted accurately, CS specimens were immersed vertically in the acid solution in the absence and presence of the inhibitor at different concentrations for 12 hours at 298 K. Solution volume was 80 ml. After the corrosion test, the specimens of steel were carefully washed in double-distilled water, dried and then weighed. The rinse removed loose segments of corroded samples' film. Triplicate experiments were performed in each case, and the mean value of weight loss is reported using an analytical balance (precision ±0.1 mg).

3. Results and Discussion

3.1. Essential oil composition

The essential oil composition of *Cupressus arizonica* is given in Table 1. The molecular structure of the most abundant compound is given in Figure 1 (melting point m.p. = 177°C, molecular weight $M = 136.234$ g·mol^{-1}, and density $d = 0.858$).

Table 1. Chemical composition of *Cupressus arizonica* essential oil (CAEO).

KI	Compounds	Composition (%)
932	α-Pinene	9.39
970	Sabinene	0.41
974	β-Pinene	0.32
984	Myrcene	0.62
1006	Δ-3-Carene	0.43
1011	1,4-Cineole	0.23
1019	*p*-Cymene	0.74
1024	Limonene	2.18
1053	γ-Terpinene	0.43
1082	*meta*-cymenene	0.63
1091	*p*-Cymenene	0.23
1107	6-Camphenol	0.22
1137	*trans*-Sabinol	0.29
1142	*cis*-Pinene hydrate	0.64
1172	Umbellulone	19.88
1177	Terpinen-4-ol	3.1
1180	*p*-Cymen-8-ol	1.64
1187	α-Terpineol	0.68
1195	*cis*-Piperitol	0.42
1208	*trans*-Piperitol	0.32
1218	*cis*-Sabinene hydrate acetate	0.25
1226	Citronellol	0.31

KI	Compounds	Composition (%)
1236	*Z*-Ociménone	0.38
1251	*trans*-Sabinene hydrate acetate	0.29
1281	α-Terpinene-7-ol	0.26
1292	δ-Terpinene-7-ol	0.65
1342	α-Terpenylacetate	0.65
1420	(*E*)-Caryophyllene	0.24
1429	β-Copaene	0.16
1449	*cis*-Muurola-3,5-diene	3.59
1470	*cis*-Muurola-4(14),5-diene	21.27
1499	α-Muurolene	7.87
1515	β-Curcumene	0.35
1525	δ-Cadinene	5.84
1539	α-Cadinene	1.32
1547	Elimol	0.4
1553	Germacrene B	0.75
1563	β-Calacorene	0.84
1586	Thyjopsan-2α-ol	0.27
1617	1,10-Di-*epi*-cubenol	0.72
1632	α-Acorenol	0.24
1641	*epi*-α-Muurolol	4.76
1652	α-Cadinol	0.96
1661	Dehydro-eudesmol	0.53
1668	*E*-Bisabolol-11-ol	0.28
1680	epi-α-Bisabolol	0.38
1687	α-Bisabolol	0.38
1701	Caryophyllene acetate	1.68
1730	Curcumenol	0.51
1759	2,7(14)-bisaboladien-12-ol	0.52

KI: Kováts indices

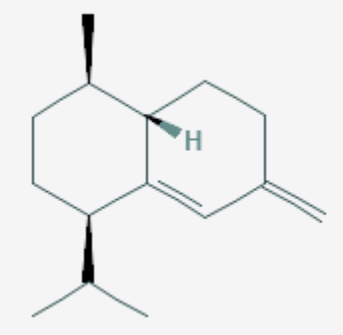

Figure 1. The molecular structure of *cis*-Muurola-4(14),5-diene.

3.2. Weight loss measurements

The values of percentage inhibition efficiency η_w (%) and the corrosion rate (*W*) obtained from weight loss method at different concentrations of CAEO at 298 K are summarized in Table 2. The corrosion rate (*W*) and inhibition efficiency η_w (%) were calculated according to equations (1) and (2), respectively [23]:

$$W_{corr} = \frac{\Delta m}{S \cdot t} \quad (1)$$

$$\eta_w\% = \frac{W_{corr} - W_{corr/inh}}{W_{corr}} \times 100 \quad (2)$$

Where Δm (mg) is the specimen's weight before and after immersion in the tested solution, W_{corr} and $W_{corr/inh}$ are the values of corrosion weight losses (mg/cm^2·h) of carbon steel in uninhibited and inhibited solutions, respectively; *S* is the area of the carbon steel specimen (cm^2) and *t* is the exposure time (h).

Table 2. Weight loss results of carbon steel in 1.0 M HCl without and with different concentrations of CAEO (t = 12 h, T = 298 K).

Inhibitor	Concentration (ppm)	W (mg·cm^{-2}·h^{-1})	η_W (%)
blank	0	0.625	–
CAEO	500	0. 017	97
	100	0.051	92
	50	0.067	89
	25	0.077	87
	12.5	0.103	83

Results in Table 2 show that the corrosion rate (W) of carbon steel significantly decreased in the presence of the inhibitor. All CAEO's concentrations show a high inhibition efficiency with a maximum value of 97% at 500 ppm. This behavior could be explained by

the adsorption of phytochemical components of the essential oil onto the mild steel surface resulting in the blocking of the reaction sites, and protection of the carbon steel surface from the attack of corrosion active ions in the acid medium [20, 24]. Thus, making CAEO an excellent corrosion inhibitor for carbon steel in 1.0 M HCl solution.

3.3. Potentiodynamic Polarization

3.3.1. Effect of concentration

The cathodic and anodic polarization curves of carbon steel in 1.0 M HCl in the absence and presence of CAEO at different concentrations and 298 K are presented in Figure 2. From these data, the presence of CAEO at different concentrations shifts the values of i_{corr} towards lower values compared to that in uninhibited solution. The shift in corrosion current density, however, is more pronounced at higher concentrations. Both cathodic and anodic branches of the curves are decreased, suggesting that CAEO affects steel dissolution and hydrogen ion simultaneously [23]. Besides, it is well-known that, if the deviation in E_{corr} is greater than 85 mV in the inhibited system with respect to uninhibited one, the inhibitor can be recognized as cathodic or anodic type. In contrast, if the deviation in E_{corr} is less than 85 mV, it can be identified as a mixed-type inhibitor [25, 26]. Here in, since the variation in E_{corr}, in our case, is lower than 85 mV. So, the inhibitor can be classified as a mixed type.

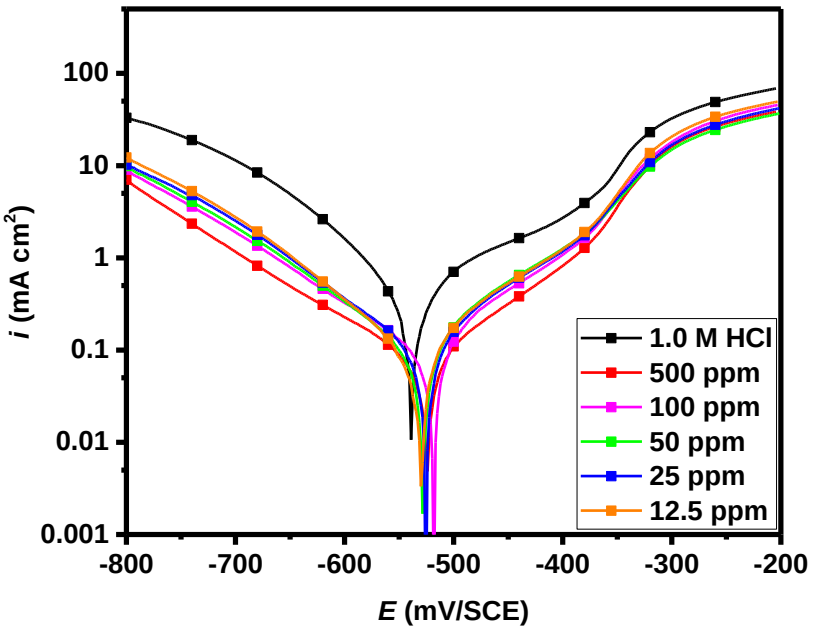

Figure 2. Cathodic and anodic polarization curves of carbon steel in 1.0 M HCl at different concentrations of CAEO at 298 K.

The values of the electrochemical parameters (corrosion potential (E_{corr}), corrosion current density (i_{corr}), cathodic Tafel slope (β_c)) at different CAEO concentrations are

reported in Table 3.The values of β_c are calculated from the linear region of the polarization curves. Inspection of results in Table 3 reveals that both anodic and cathodic slopes are approximately constant, suggesting, therefore that the inhibiting action is mainly based on a purely blocking mechanism [27]. Thus, all the calculations in our study were based on this assumption. The i_{corr} is determined from the intersection of the linear part of cathodic curves with the corresponding stationary corrosion potential. The inhibition efficiency is evaluated from i_{corr} values using the relationship (3) [23]:

$$\eta_{PDP}\% = \frac{i_{corr}^{0} - i_{corr}^{inh}}{i_{corr}^{0}} \times 100 \quad (3)$$

Where i_{corr}^{0} and i_{corr}^{inh} are the corrosion current densities in the absence and presence of CAEO inhibitor, respectively determined by extrapolation of cathodic Tafel lines to E_{corr}.

Table 3. Electrochemical parameters of carbon steel at various concentrations of CAEO in 1.0 M HCl and corresponding inhibition efficiencies.

Inhibitor	**Concentration ppm**	$-E_{corr}$ **mV/SCE**	i_{corr} **μA·cm^{-2}**	$-\beta_c$ **mV·dec^{-1}**	β_a **mV·dec^{-1}**	η_{PDP} **%**
Blank	–	535	634	128	133	–
CAEO	500	527	52	132	123	92
	100	518	70	136	124	89
	50	530	95	133	127	85
	25	525	105	130	126	82
	12.5	532	118	126	121	81

Cathodic current-potential curves give rise to parallel Tafel lines, which indicate that hydrogen evolution reaction is not controlled and that the addition of CAEO does not modify the mechanism of this process [28, 29]. The displayed data in Table 3 shows that the presence of CAEO decreases the i_{corr} from 634 (Blank) to 50 μA cm^2 at 500 ppm with an inhibition efficiency of 92%. The higher inhibition effect achieved at all concentrations suggests that tested essential oil is an effective corrosion inhibitor in acidic media.

3.3.2. Effect of Temperature

To evaluate the effect of temperature on carbon steel corrosion, PDP measurements were also performed at a temperature range of 298–328 K in the absence and presence of the studied inhibitor. Results are listed in Table 4 and Figure 3, from which we observed that with increasing the solution temperature, the corrosion rate was increased in both inhibited and uninhibited electrolytes. This causes a decrease in the corrosion inhibition performance of the tested essential oil. Evidently, this is due to a reduction in adsorption tendency of CAEO's molecules on the carbon steel surface [30]. It is well known that, at higher

temperatures, inhibitor molecules possess high kinetic energy, which affects their adsorption, and mainly molecular disintegration, rapid etching, and re-arrangement could also occur at such conditions [31, 32].

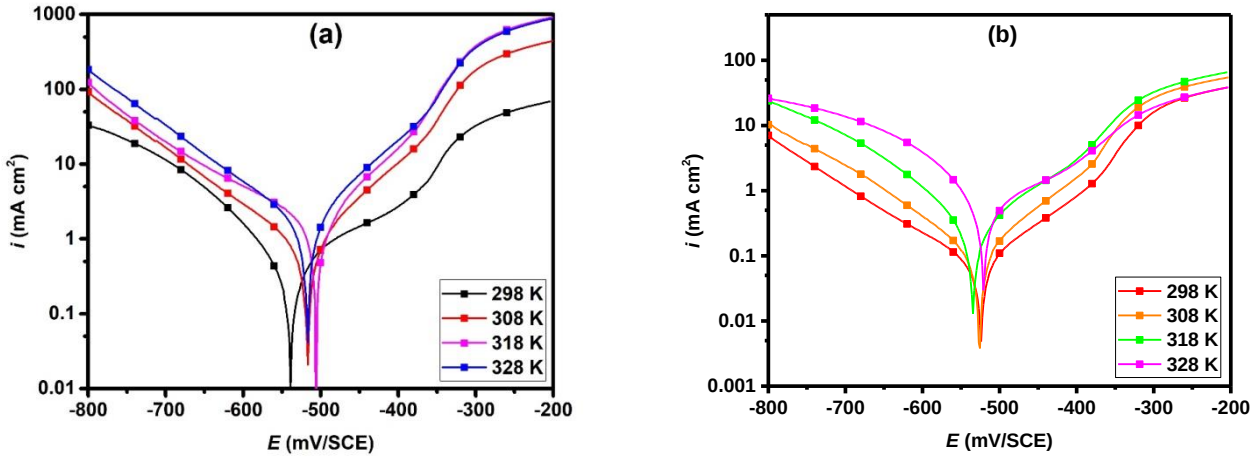

Figure 3. Potentiodynamic polarization curves for corrosion of carbon steel in (a) 1.0 M HCl solution and in (b) the presence of 500 ppm at different temperatures.

Table 4. Corrosion parameters obtained from potentiodynamic polarization of carbon steel in 1.0 M HCl with and without addition of various concentrations of CAEO at different temperatures.

Medium	Temperature (K)	i_{corr} (μA·cm^{-2})	$-E_{corr}$ (mV/SCE)	η_{PDP} (%)
Blank	298	634	535	–
	308	783	516	–
	318	992	506	–
	328	1372	517	–
CAEO	298	50	527	92
	308	111	526	86
	318	205	535	79
	328	387	521	72

The corrosion reaction can be considered as an Arrhenius form process following the equation below [31]:

$$i_{corr} = A\exp\left(-\frac{E_a}{RT}\right) \quad (4)$$

Where E_a is the apparent activation energy of the corrosion process, R is the universal gas constant, T is the absolute temperature and A is the Arrhenius pre-exponential factor.

Figure 4 shows Arrhenius plots (log i_{corr} *vs* 1/*T*) for carbon steel in blank solution and the presence of 500 ppm of CAEO at different temperatures. The activation energies were found to be 20.65 and 54.65 kJ/mol for 1.0 M HCl alone and in the presence of 500 ppm of CAEO, respectively. The increase in activation energy after addition of CAEO to 1.0 M HCl indicates an increase in the energy barrier for the corrosion of carbon steel [31, 32].

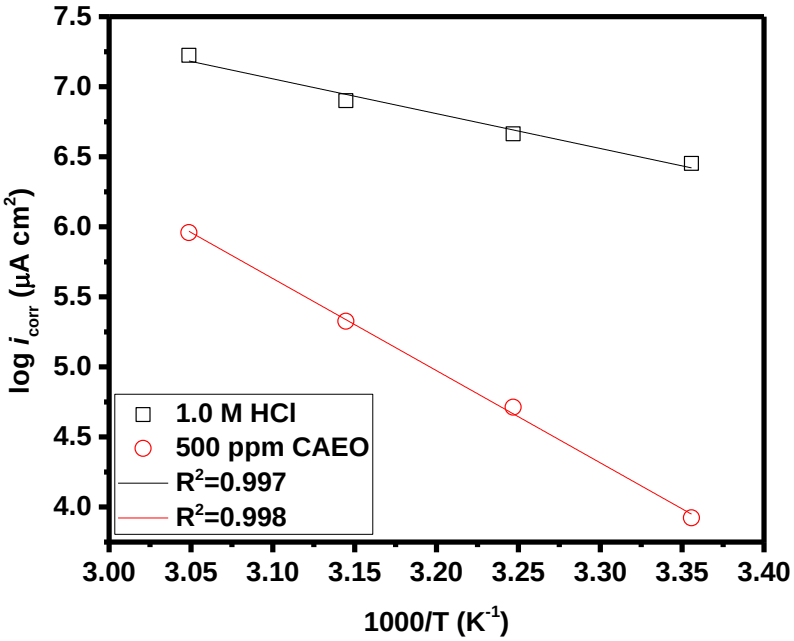

Figure 4. Arrhenius plots of log (i_{corr}) *vs.* 1/*T* for carbon steel in the absence and presence of 500 ppm of CAEO.

3.4. EIS measurements

The impedance spectroscopy could be used as a powerful technique to characterize the corrosion parameters at metal/electrolyte interface [33, 34]. Figure 5 represents Nyquist, Bode, and phase angle plots obtained at 298 K. The inhibition efficiency obtained from EIS measurements (η_{EIS}%) can be calculated by the following equation 5:

$$\eta_{EIS}\% = \frac{R_{p/inh} - R_p}{R_{p/inh}} \times 100 \quad (5)$$

Where $R_{p/inh}$ and R_p are the polarization resistances in inhibited and uninhibited solutions, respectively.

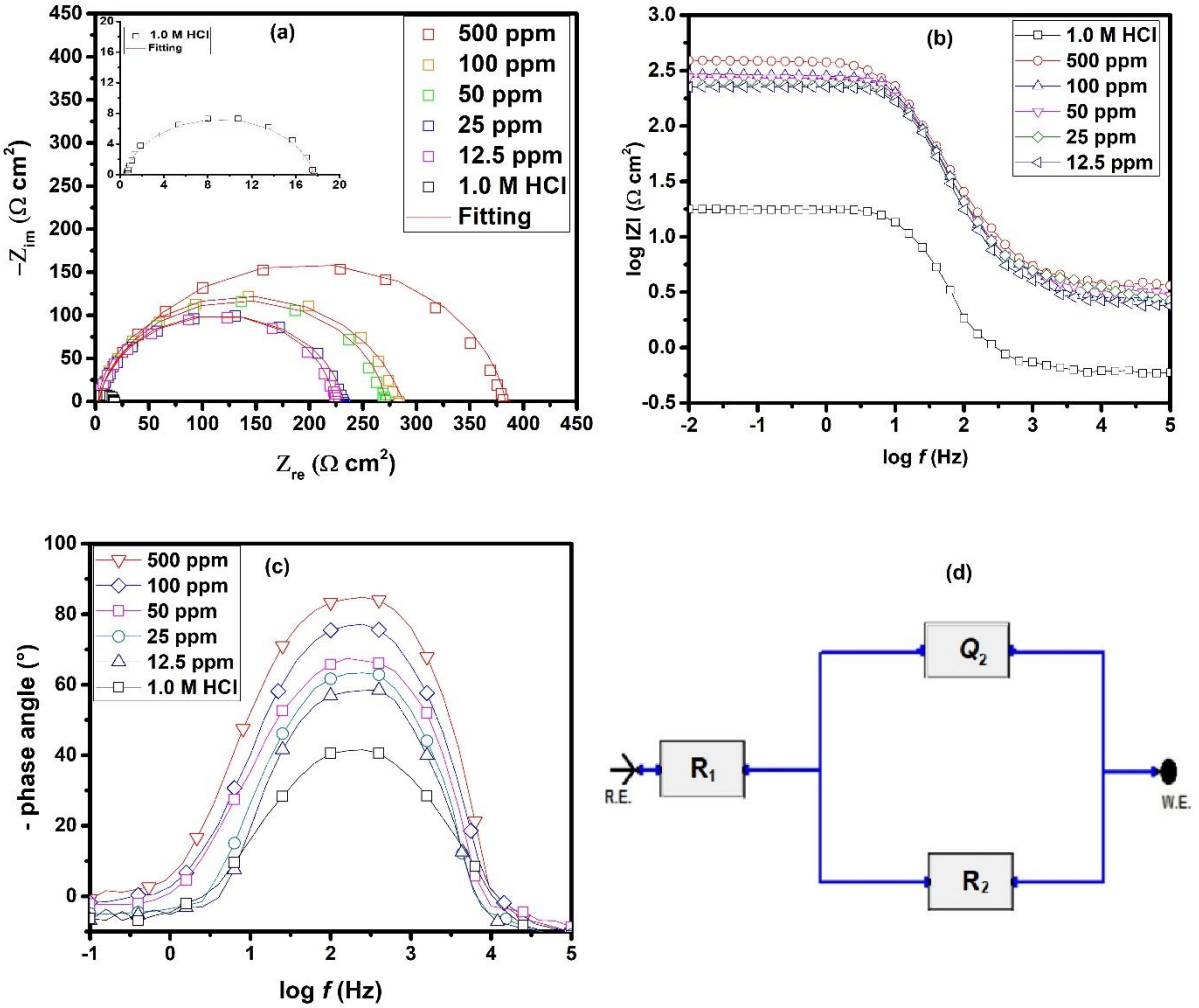

Figure 5. Nyquist diagrams for carbon steel electrode with and without CAEO after 30 min of immersion in 1.0 M HCl at 298 K.

From the results in Figure 5(a), it is observed that all corresponding impedance diagrams are characterized by a single capacitive loop and are similar in shape. This observation indicates that the corrosion of carbon steel in 1.0 M HCl solution is mainly controlled by the charge transfer process [33, 35]. It is clear that the diameter of the impedance spectra increases upon the concentration of CAEO increased, which could be explained by the rise in the charge transfer resistances [31, 34].

Taking into account heterogeneity and roughness of carbon steel electrodes, a constant phase element (CPE) was employed to fit the non-ideal capacitive behavior in the equivalent circuit used for the fitting of impedance data (Figure 5(d)) [1, 23]. It includes a CPE and a polarization resistance R_p, parallels to it. These both components are in series with solution resistance; R_s. All electrochemical parameters extracted using the equivalent circuit are listed in Table 5.

From the impedance parameters, one can observe that the value of R_p increases with the presence of CAEO, which causes a decrease in the double-layer capacitance. If one assumes that the double layer between the charged surface and the electrolyte is considered as an electrical capacitor, the adsorption of CAEO on the electrode may decrease the electrical capacity because the inhibitor displaces the water molecules or even others ions initially adsorbed on the electrode [36]. Thus, the decrease in C_{dl} values with the rise of CAEO concentration confirms the effective adsorption of CAEO's molecules on the surface of the carbon steel [31, 36]. Therefore, better protection of steel surface against corrosion could be achieved. These results are supported by higher inhibition efficiencies at all CAEO's concentrations, reaching a maximum value of 95% at 500 ppm.

Table 5. Electrochemical parameters of carbon steel at various concentrations of CAEO in 1.0 M HCl and corresponding inhibition efficiencies.

Inhibitor	**Concentration (ppm)**	R_s **(Ω·cm²)**	R_p **(Ω·cm²)**	C_{dl} **(μF·cm⁻²)**	***n***	Q **(μF·S^{n-1})**	η_{EIS} **(%)**
Blank	–	3.09	17.5	126.32	0.892	244.50	–
CAEO	500	3.62	377	19.14	0.902	31.03	95
	100	2.46	279	22.42	0.915	34.52	94
	50	3.48	268	26.84	0.914	41.03	93
	25	3.46	227	28.51	0.924	41.82	92
	12.5	3.03	216	29.65	0.926	43.09	91

Conclusion

This work reported the corrosion inhibition behavior of the essential oil of *Cupressus arizonica* for carbon steel in 1.0 M HCl. The principal constituent of (CAEO) is *cis*-Muurola-4(14),5-diene (21.27%). Results indicated that the essential oil of *Cupressus arizonica* acts as a good carbon steel corrosion inhibitor in hydrochloric acid. In all experimental methods, the inhibition efficiency increased with the rise in CAEO's concentration and attained a maximum value of 95% at 500 ppm. PDP results revealed that the *Cupressus arizonica* leaves essential oil acted as a mixed-type inhibitor. EIS results suggested that CAEO inhibits carbon steel corrosion by the adsorption process.

Acknowledgements

We are grateful and thankful to Dr. Manal Naciri, University Mohamed V. in Rabat for her help given for improving in electrochemical experiments.

References

1. Y. El Aoufir, R. Aslam, F. Lazrak, R. Marzouki, S. Kaya, S. Skal, A. Ghanimi, I.H. Ali, A. Guenbour, H. Lgaz and I.-M. Chung, The effect of the alkyl chain length on corrosion inhibition performances of 1, 2, 4-triazole-based compounds for mild steel in 1.0 M HCl: Insights from experimental and theoretical studies, *J. Mol. Liq*., 2020, **303**. doi: 10.1016/j.molliq.2020.112631
2. A.K. Singh, S. Thakur, B. Pani, B. Chugh, H. Lgaz, I.-M. Chung, P. Chaubey, A.K. Pandey and J. Singh, Solvent-free microwave assisted synthesis and corrosion inhibition study of a series of hydrazones derived from thiophene derivatives: Experimental, surface and theoretical study, *J. Mol. Liq*., 2019, **283**, 788–803. doi: 10.1016/j.molliq.2019.03.126
3. G. Trabanelli, Whitney award lecture: inhibitors – an old remedy for a new challenge, *Corrosion*, 1991, **47**, no. 6, 410–419. doi: 10.5006/1.3585271
4. A. Satapathy, G. Gunasekaran, S. Sahoo, K. Amit and P. Rodrigues, Corrosion inhibition by *Justicia gendarussa* plant extract in hydrochloric acid solution, *Corros. Sci*., 2009, **51**, no. 12, 2848–2856. doi: 101016/jcorsci.2009.08.016
5. A. Chaouiki, H. Lgaz, R. Salghi, M. Chafiq, H. Oudda, Shubhalaxmi, K.S. Bhat, I. Cretescu, I.H. Ali, R. Marzouki and I.-M. Chung, Assessing the impact of electron-donating-substituted chalcones on inhibition of mild steel corrosion in HCl solution: Experimental results and molecular-level insights, *Colloids Surf. Physicochem. Eng. Asp*., 2020, **588**. doi: 10.1016/j.colsurfa.2019.124366
6. A. Singh, K.R. Ansari, D.S. Chauhan, M.A. Quraishi, H. Lgaz and I.-M. Chung, Comprehensive investigation of steel corrosion inhibition at macro/micro level by ecofriendly green corrosion inhibitor in 15% HCl medium, *J. Colloid Interface Sci*., 2020, **560**, 225–236. doi: 10.1016/j.jcis.2019.10.040
7. R. Kumar, S. Chahal, S. Kumar, S. Lata, H. Lgaz, R. Salghi and S. Jodeh, Corrosion inhibition performance of chromone-3-acrylic acid derivatives for low alloy steel with theoretical modeling and experimental aspects, *J. Mol. Liq*., 2017, **243**, 439–450. doi: 10.1016/j.molliq.2017.08.048
8. A. Singh, K.R. Ansari, J. Haque, P. Dohare, H. Lgaz, R. Salghi and M.A. Quraishi, Effect of electron donating functional groups on corrosion inhibition of mild steel in hydrochloric acid: Experimental and quantum chemical study, *J. Taiwan Inst. Chem. Eng*., 2018, **82**, 233–251. doi: 10.1016/j.jtice.2017.09.021
9. V.V. Torres, R.S. Amado, C.F. De Sá, T.L. Fernandez, C.A. da Silva Riehl, A.G. Torres and E. D'Elia, Inhibitory action of aqueous coffee ground extracts on the corrosion of carbon steel in HCl solution, *Corros. Sci*., 2011, **53**, 2385–2392. doi: 10.1016/j.corsci.2011.03.021
10. C. Verma, E.E. Ebenso, M.A. Quraishi, Alkaloids as green and environmental benign corrosion inhibitors: An overview, *Int. J. Corros. Scale Inhib*., 2019, **8**, 512–528. doi: 10.17675/2305-6894-2019-8-3-3

11. V.I. Vorobyova, M.I. Skiba, I.M. Trus, Apricot pomaces extract (*Prunus armeniaca l.*) as a highly efficient sustainable corrosion inhibitor for mild steel in sodium chloride solution, *Int. J. Corros. Scale Inhib*., 2019, **8**, no. 4,1060–1083. doi: 10.17675/2305-6894-2019-8-4-15
12. M. Barrahi, H. Elhartiti, A. El Mostaphi, N. Chahboun, M. Saadouni, R. Salghi, A. Zarrouk and M. Ouhssine, Corrosion inhibition of mild steel by fennel seeds (*Foeniculum vulgare mill*) essential oil in 1 M hydrochloric acid solution, *Int. J. Corros. Scale Inhib*., 2019, **8**, no. 4, 937–953. doi: 10.17675/2305-6894-2019-8-4-9
13. B. Hafez, M. Mokhtari, H. Elmsellem and H. Steli, Environmentally friendly inhibitor of the corrosion of mild steel: Commercial oil of eucalyptus, *Int. J. Corros. Scale Inhib*., 2019, **8**, no. 3, 573–585. doi: 10.17675/2305-6894-2019-8-3-8
14. B.N. Subedi, K. Amgain, S. Joshi and J. Bhattarai, Green approach to corrosion inhibition effect of *vitex negundo* leaf extract on aluminum and copper metals in biodiesel and its blend, *Int. J. Corros. Scale Inhib*., 2019, **8**, 744–759. doi: 10.17675/2305-6894-2019-8-3-21
15. S. Bouazama, J. Costat, J.M. Desjobertb, A. Benali, A. Guenbour and M. Tabyaoui, Influence of *lavandula dentata* essential oil on the corrosion inhibition of carbon steel in 1 M HCl solution, *Int. J. Corros. Scale Inhib*., 2019, **8**, no. 1, 25–41. doi: 10.17675/2305-6894-2019-8-1-3
16. A. Boukhraz, A. Chaouik, R. Salghi, H. Elhartiti, N. Saouide el Ayne, A. Zaher and M. Ouhssine, Inhibitive effect of *Thymus satureioides* essential oil as a green corrosion inhibitor for mild steel in an acidic medium, *Int. J. Corros. Scale Inhib*., 2019, **8**, no. 1, 291–305. doi: 10.17675/2305-6894-2019-8-2-11
17. H.E. Hartiti, A. Elmostaphi, M. Barrahi, M. Saadouni, R. Salghi, A. Zarrouk, B. Bourkhiss and M. Ouhssine, Valorization of the essential oil of *myrtus communis* by its use as a corrosion inhibitor of mild steel in acidic medium 1.0 M HCL, *Int. J. Corros. Scale Inhib*., 2019, **8**, no. 4, 1084–1096. doi: 10.17675/2305-6894-2019-8-4-16
18. F. El Hajjaji, H. Greche, M. Taleb, A. Chetouani, A. Aouniti and B. Hammouti, Application of essential oil of *thyme vulgaris* as green corrosion inhibitor for mild steel in 1 M HCl, *J. Mater. Environ. Sci*., 2016, **7**, no. 2, 566–578.
19. Y. El Ouadi, N. Lahhit, A. Bouyanzer, L. Majidi, H. Elmsellem, K. Cherrak, A. Elyoussfi, B. Hammouti and J. Costa, Chemical composition and inhibitory effect of essential oil of lavande (*Lavandula dentata*) LD on the corrosion of mild steel in hydrochloric acid (1 M), *Arab. J. Chem. Environ. Res*., 2015, **1**, no. 2, 49–65.
20. S. Andreani, M. Znini, J. Paolini, L. Majidi, B. Hammouti, J. Costa and A. Muselli, Study of corrosion inhibition for mild steel in hydrochloric acid solution by *Limbarda crithmoides* (*L.*) essential oil of Corsica, *J. Mater. Environ. Sci*., 2016, **7**, 187–195.
21. M. Manssouri, Y. El Ouadi, M. Znini, J. Costa, A. Bouyanzer, J. Desjobert and L. Majidi, Adsorption proprieties and inhibition of mild steel corrosion in HCl solution by the essential oil from fruit of Moroccan *Ammodaucus leucotrichus*, *J. Mater. Environ. Sci*., 2015, **6**, 631–646.

22. J. Clevenger, Apparatus for the determination of volatile oil, *J. Am. Pharm. Assoc*., 1928, **17**, 345–349.
23. H. Lgaz, S.K. Saha, A. Chaouiki, K.S. Bhat, R. Salghi, P. Banerjee, I.H. Ali, M.I. Khan and I.-M. Chung, Exploring the potential role of pyrazoline derivatives in corrosion inhibition of mild steel in hydrochloric acid solution: Insights from experimental and computational studies, *Constr. Build. Mater*., 2020, **233**, doi: 10.1016/j.conbuildmat.2019.117320
24. G. Cristofari, M. Znini, L. Majidi, A. Bouyanzer, S. Al-Deyab, J. Paolini, B. Hammouti and J. Costa, Chemical composition and anti-corrosive activity of *Pulicaria mauritanica* essential oil against the corrosion of mild steel in 0.5 M H_2SO_4, *Int. J. Electrochem. Sci*., 2011, **6**, 6699–6717.
25. L. Afia, R. Salghi, L. Bammou, E. Bazzi, B. Hammouti, L. Bazzi and A. Bouyanzer, Anti-corrosive properties of Argan oil on C38 steel in molar HCl solution, *J. Saudi Chem. Soc*., 2014, **18**, 19–25.
26. W. Li, Q. He, S. Zhang, C. Pei and B. Hou, Some new triazole derivatives as inhibitors for mild steel corrosion in acidic medium, *J. Appl. Electrochem*., 2008, **38**, 289–295. doi: 10.1007/s10800-007-9437-7
27. I. Zaafarany and H.A. Ghulman, Ethoxylated fatty amines as corrosion inhibitors for carbon steel in hydrochloric acid solutions, *Int. J. Corros. Scale Inhib*., 2013, **2**, no. 2, 82–91. doi: 10.17675/2305-6894-2013-2-2-082-091
28. R.K. Gupta, M. Malviya, K.R. Ansari, H. Lgaz, D.S. Chauhan and M.A. Quraishi, Functionalized graphene oxide as a new generation corrosion inhibitor for industrial pickling process: DFT and experimental approach, *Mater. Chem. Phys*., 2019, **236**, 121727. doi: 10.1016/j.matchemphys.2019.121727
29. M. Chafiq, A. Chaouiki, H. Lgaz, R. Salghi, K.V. Bhaskar, R. Marzouki, K.S. Bhat, I.H. Ali, M.I. Khan and I.-M. Chung, Inhibition performances of spirocyclopropane derivatives for mild steel protection in HCl, *Mater. Chem. Phys*., 2020, **243**, doi: 10.1016/j.matchemphys.2019.122582
30. P. Dohare, M.A. Quraishi, C. Verma, H. Lgaz, R. Salghi and E.E. Ebenso, Ultrasound induced green synthesis of pyrazolo-pyridines as novel corrosion inhibitors useful for industrial pickling process: Experimental and theoretical approach, *Results Phys*., 2019, **13**, 102344. doi: 10.1016/j.rinp.2019.102344
31. C. Verma, A.A. Sorour, E.E. Ebenso and M.A. Quraishi, Inhibition performance of three naphthyridine derivatives for mild steel corrosion in 1 M HCl: Computation and experimental analyses, *Results Phys*., 2018, **10**, 504–511. doi: 10.1016/j.rinp.2018.06.054
32. A. Mishra, C. Verma, H. Lgaz, V. Srivastava, M.A. Quraishi and E.E. Ebenso, Synthesis, characterization and corrosion inhibition studies of N-phenyl-benzamides on the acidic corrosion of mild steel: Experimental and computational studies, *J. Mol. Liq*., 2018, **251**, 317–332. doi: 10.1016/j.molliq.2017.12.011
33. M. Messali, M. Larouj, H. Lgaz, N. Rezki, F.F. Al-Blewi, M.R. Aouad, A. Chaouiki, R. Salghi and I.-M. Chung, A new schiff base derivative as an effective corrosion

inhibitor for mild steel in acidic media: Experimental and computer simulations studies, *J. Mol. Struct*., 2018, **1168**, 39–48. doi: 10.1016/j.molstruc.2018.05.018

34. D.I. Njoku, Y. Li, H. Lgaz and E.E. Oguzie, Dispersive adsorption of *Xylopia aethiopica* constituents on carbon steel in acid-chloride medium: A combined experimental and theoretical approach, *J. Mol. Liq.*, 2018, **249**, 371–388. doi: 10.1016/j.molliq.2017.11.051
35. A. Singh, K.R. Ansari, M.A. Quraishi, H. Lgaz and Y. Lin, Synthesis and investigation of pyran derivatives as acidizing corrosion inhibitors for N80 steel in hydrochloric acid: Theoretical and experimental approaches, *J. Alloys Compd*., 2018, **762**, 347–362. doi: 10.1016/j.jallcom.2018.05.236
36. W. Emori, R.-H. Zhang, P.C. Okafor, X.-W. Zheng, T. He, K. Wei, X.-Z. Lin and C.-R. Cheng, Adsorption and corrosion inhibition performance of multi-phytoconstituents from *Dioscorea septemloba* on carbon steel in acidic media: Characterization, experimental and theoretical studies, *Colloids Surf., A.*, 2020, **590**, 124534. doi: 10.1016/j.colsurfa.2020.124534

♦ ♦ ♦